Bioresource Technology 247 (2018) 553–560

Contents lists available at ScienceDirect

Bioresource Technology

journal homepage: www.elsevier.com/locate/biortech

Genome hunting of carbonyl reductases from *Candida glabrata* for efficient preparation of chiral secondary alcohols

Guochao Xu, Yaping Zhang, Yue Wang, Ye Ni*

The Key Laboratory of Industrial Biotechnology, Ministry of Education, School of Biotechnology, Jiangnan University, Wuxi 214122, Jiangsu, China

GRAPHICAL ABSTRACT

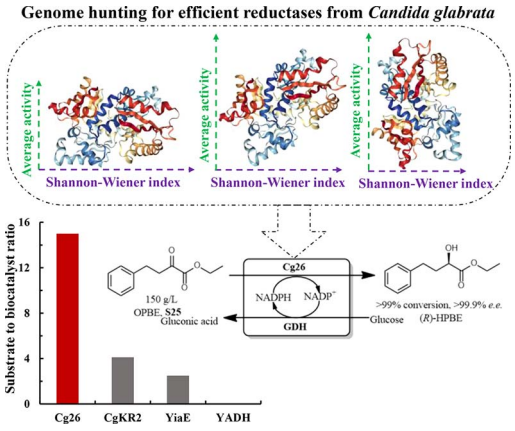

ARTICLE INFO

Keywords:
Candida glabrata
Genome hunting
Reductase
Chiral secondary alcohol
Shannon-Wiener index

ABSTRACT

In this work, genome hunting strategy was adopted in screening for reductases from *Candida glabrata*. A total of 37 putative reductases were successfully expressed in *E. coli* BL21(DE3). A substrate library containing 32 substrates was established for characterization of each reductase by average specific activity and Shannon-Wiener index. Among them, Cg26 was identified with the highest efficiency and wider substrate spectrum in the reduction of prochiral ketones, with average activity and Shannon-Wiener index of 8.95 $U \cdot mg^{-1}$ and 2.82. Cg26 is a member of 'extended' short chain dehydrogenase/reductase superfamily. Ni^{2+} could improve its activity. As much as 150 $g \cdot L^{-1}$ ethyl 2-oxo-4-phenylbutyrate could be completely converted by 10 $g \cdot L^{-1}$ Cg26. This study provides evidence for this newly identified Cg26 in the preparation of chiral secondary alcohols.

1. Introduction

Optically pure secondary alcohols are one class of the most important chiral compounds, and have been widely applied as building blocks in the fine chemicals, pharmaceutical, materials, agrochemicals and food industries (Zheng and Xu 2011). The efficient and economic synthesis of chiral secondary alcohols is of special interest. Various strategies have been developed for the production of single enantiomer of secondary alcohols, including chromatographic separation, enantioselective resolution or dynamic kinetic resolution, and asymmetric reduction (Zheng et al., 2017). In the view of atomic economy, product yield, operational simplicity and enantioselectivity, chemically or

* Corresponding author.
E-mail address: yni@jiangnan.edu.cn (Y. Ni).

http://dx.doi.org/10.1016/j.biortech.2017.09.111
Received 30 July 2017; Received in revised form 13 September 2017; Accepted 15 September 2017
Available online 20 September 2017

biocatalytically asymmetric hydrogenation of prochiral ketones is regarded as the most promising strategy (Goldberg et al., 2007; Matsuda et al., 2009; Huisman et al., 2010).

It is widely accepted that chemical reduction plays important role in the industrial synthesis of chiral secondary alcohols with high efficiency, however at the expense of environmental friendliness and toxicity (Kroutil et al., 2004). In addition, high enantioselectivity is often difficult to achieve by chemical routes. Biocatalytically asymmetric reduction is regarded as an alternative for chemical methods, and presents many appealing features, such as gentle reaction conditions, high activity and stereoselectivity, no need of protection and deprotection steps (Zheng et al., 2017). However, the narrow substrate profile, low substrate/product tolerance, and demand for cofactor NAD(P)$^+$ render their application less satisfactory (Itoh, 2014). As a result, there is a constant need for discovering novel biocatalysts with diverse properties, such as wide substrate scope, high activity, enantioselectivity and thermostability etc, by searching for naturally evolved enzymes, protein engineering and *de novo* design of new biocatalysts (Ni and Xu, 2012). Over the past decade, an increasing number of chemists have turned to biocatalysis in their synthetic schemes, especially in the context of great advances in genomics and protein databases, screening, and evolution technologies (Bornscheuer et al., 2012).

Genome hunting is one of the genome mining strategies for screening naturally evolved biocatalysts, and is performed by screening a genome-wide expression library of a certain microorganism with desired activity, which can be developed by overexpressing the known or putative reductases (Ni and Xu, 2012). A large number of naturally evolved reductases have been discovered through this strategy in recent years. One typical example of genome hunting is the systematic investigation on reductases from *Saccharomyces cerevisiae*, a well-known reductases producing strain. After analysis and characterization, many reductases displayed > 90% *e.e.* in the reducing of *α*- or *β*-keto esters, and the utility of this library was further demonstrated by reducing 3-oxo-3-phenylpropanenitrile to its corresponding alcohol with high enantioselectivity (Kaluzna et al., 2004). Genome hunting library of *Bacillus* sp. ECU0013, a reductase-producing strains, has also been developed and screened for useful reductases, and three versatile reductases were identified with application potential in efficient synthesis of optically active *α*- and *β*-hydroxyl esters (Ni et al., 2011). Comparative characterization of ene-reductases library of cyanobacteria revealed 9 ene-reductases with higher catalytic efficiency and enriched the toolbox for the asymmetric reduction of alkenes (Fu et al., 2013). Bioinformatics analysis based on sequence-similarity with an anti-Prelog stereospecific ADH from *Candida parapsilosis* in its whole genome returned three carbonyl reductases with reducing activity toward 2-hydroxyacetophenone (Nie et al., 2011).

Candida glabrata, previously known as *Torulopsis glabrata*, is a haploid yeast of the genus Candida and regarded as an important industrial microorganism, with potential in fermentation for acetoin (Li et al., 2015), pyruvate (Li et al., 2001; Otto et al., 2011), malate (Chen et al., 2013) and fumarate (Chen et al., 2015) etc. *C. glabrata* have been proved to be efficient in the asymmetric reduction of 2-oxo-4-phenylbutanate (OPBE) (Zhang et al., 2009), and is also a reductase-producing strain. Three reductases have been identified, including *Cg*KR1 for ethyl (*R*)-*o*-chloromandelate (Ma et al., 2012), *Cg*KR2 for ethyl (*R*)-2-hydroxy-4-phenylbutyrate (HPBE) (Shen et al., 2012) and *Cg*CR for (*R*)-halohydrins (Xu et al., 2015). We thus supposed to introduce the screening criteria of height and breadth in substrate spectrum in order to screening the genome hunting library of *C. glabrata* for reductases with wide substrate spectrum, high activity and enantioselectivity. The genome hunting library of *C. glabrata* containing all putative reductases were developed and comparatively studied by average activity and Shannon-Wiener index toward substrate library containing 32 substrates (Fig. 1). The enzymatic properties and application potentials of the best reductase in the preparation of chiral secondary alcohols were also investigated.

2. Material and methods

2.1. Chemical reagents, plasmid and strain

All prochiral ketones, aldehyde and alkene substrates for reductases were purchased from Aladdin Co. (Shanghai). Cofactors NAD(P)$^+$ and NAD(P)H were bought from Bontac Bio-engineering Co. (Shenzhen). Other reagents were purchased from Sinopharm Co. (Shanghai) unless otherwise stated. Plasmid pET28a and *Escherichia coli* BL21(DE3) were stored in our lab.

2.2. Cloning and expression of reductases from Candida glabrata

Genomic DNA of *C. glabrata* was extracted using column genomic DNA extraction kit GK0122 (Shanghai Generay Biotech Co.) and used as template. Fifty-five putative reductase coding genes with length at range of 600–1500 bp were amplified using KOD polymerase (Toyobo Life Science Co., Shanghai) and primers listed in E-supplement from genomic DNA of *C. glabrata*. Vector pET28a was double digested with *Bam*H I and *Sal* I. The resultant PCR products were ligated into the linearized pET28a using Exnase II (Vazyme Co., Nanjing). The recombinant plasmids were transferred into *E. coli* BL21(DE3) and verified by colony PCR and sequencing. Heterogeneous expression of the reductases were performed by inoculated the recombinant *E. coli* BL21(DE3) in LB medium with 50 μg·mL^{-1} kanamycin and cultured at 37 °C and 180 rpm, and 0.2 mM isopropyl-β-D-thiogalactoside (IPTG) was supplemented when the OD_{600} reached 0.6–0.8 and further cultivated at 25 °C and 180 rpm for 6 h. The cells were collected by centrifuge at 8000 × *g* and 4 °C for 5 min, washed twice with physiological saline, re-suspended with phosphate sodium buffer (pH 7.0, 100 mM) and disrupted twice by high pressure homogenization at 600–800 bar (AH-BASICI, ATS Engineering Inc, Shanghai). The supernatant was obtained by centrifuge at 8000 × *g* and 4 °C for 20 min. SDS-PAGE analysis was performed to examine the expression level of all the recombinant reductases (E-supplement).

2.3. Activity assay

Standard enzyme activity assay protocol was spectrophotometrically performed by monitoring the absorbance changes of NADH or NADPH at 340 nm. The reaction mixture consisted of 2 mM substrate, 0.5 mM NADH or NADPH in 190 μL PBS buffer (pH 7.0, 100 mM) and 10 μL enzyme solution with appropriated concentration at 30 °C. The molar extinction coefficient of NADH or NADPH was 6220 L·mol^{-1}·cm^{-1}. One unit of reductase activity was defined as the amount of reductase that catalyzed the oxidation of 1 μmol NADH or NADPH per minute under above mentioned condition. Protein concentration was determined using Bradford method with BSA as standard protein. The specific activity of reductases was calculated according to Eq. (1).

$$\text{Activity (U/mL)}\frac{\Delta OD_{340} \times V \times 10^3}{6220 \times l}\text{, Specific activity (U/mg)} = \frac{\text{Activity (U/mL)}}{\text{Protein concentration (mg/mL)}} \quad (1)$$

where ΔOD_{340} is the absorbance changes at 340 nm per minute, V is the reaction volume (mL), l is the optical path length (cm).

2.4. Shannon-Wiener index

The Shannon-Wiener index was used as a diversity index in the statistic and adopted to describe the breadth of substrate spectrum of enzymes (Liu et al., 2013). The Shannon-Wiener index was calculated according to Eq. (2).

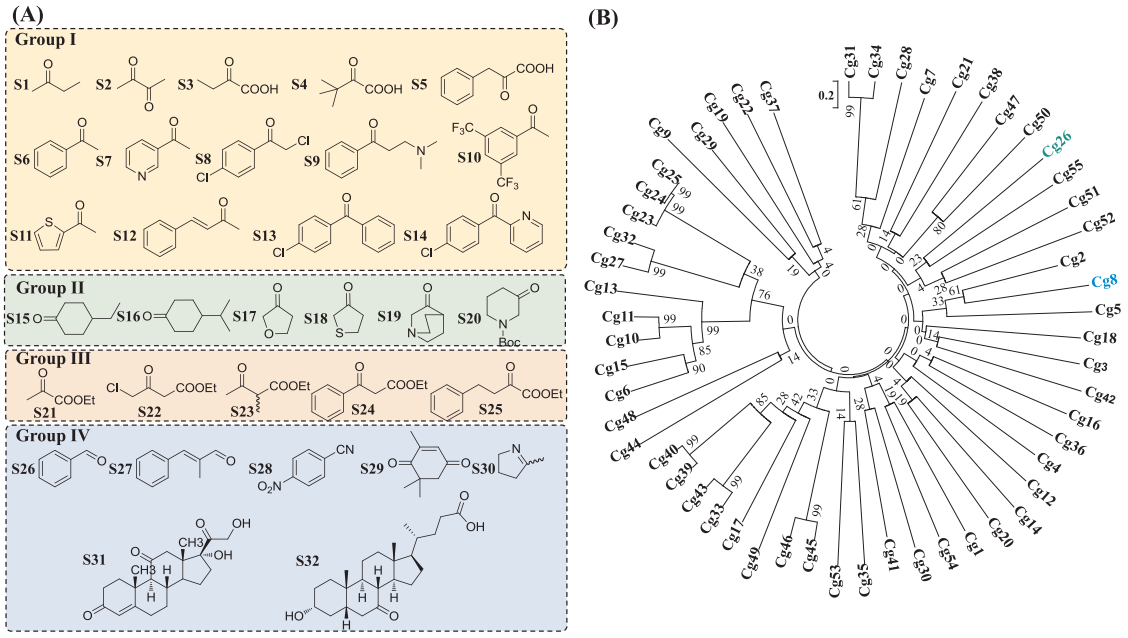

Fig. 1. Substrates applied for the characterization of reductases (A) and phylogenetic analysis of all the putative reductases from hunting library of *Candida glabrata* (B).

$$\text{Shannon-Wiener index} = -\sum_{i=1}^{n} P\text{si} \times \ln P\text{si}, \quad P\text{si} = \frac{Asi}{A} \tag{2}$$

where n is the sum of all the tested substrates, A_{si} is the specific activity of enzyme toward one substrate (si), A is the sum of specific activities of enzyme toward all the tested substrates.

2.5. Primary screening of the hunting library

Primary screening of the hunting library of *C. glabrata* was performed by testing the activity of all the overexpressed reductase toward diverse substrates as shown in Fig. 1. Activity assay was performed using the protocol as above mentioned excepted for the different substrates. The average specific activity and Shannon-Wiener index were calculated based on the specific activities of each reductase toward each substrate. All the assays were performed in triplicate.

2.6. Protein purification

Recombinant *E. coli* BL21(DE3) harboring Cg8 and Cg26 were harvested, washed and re-suspended in buffer A (20 mM PBS, 1.0 M NaCl, 20 mM imidazole, pH 7.4), followed by disruption using high pressure homogenizer as above described. The lysates were centrifuged at 4 °C and 12,000 × *g* for 20 min and filtrated with 0.2 μm filter. The resultant supernatant was loaded onto a Histrap FF column (1 mL) which was equilibrated with buffer A. Recombinant Cg8 and Cg26 were eluted from the column with an increasing imidazole gradient from 10 to 500 mM with buffer B (20 mM PBS, 1.0 M NaCl, 500 mM imidazole, pH 7.4) at a flow rate of 1 mL·min^{-1} and 4 °C. All the collected eluents were analyzed by SDS-PAGE and the eluents containing purified proteins were desalted and concentration at 4 °C. The purity of the Cg8 and Cg26 were determined by SDS-PAGE, and stored at −80 °C with 20% glycerol for further use.

2.7. Enzyme characterization

Substrate spectrum of the purified Cg8 and Cg26 were determined using above mentioned standard activity assay protocol against 32 substrates, which was divided into four subgroups based on the substituents. The average specific activity and Shannon-Wiener index toward each subgroups were calculated and compared.

Effect of pH and temperature on the activities of Cg26 was also conducted with ethyl 2-oxo-4-phenylbutyrate (**S25**) and 0.5 mM NADPH as substrates under above described condition except in the following buffers (final concentration 100 mM): sodium citrate (pH 4.0–6.0), sodium phosphate buffer (pH 6.0–8.0), Glycine-NaOH (pH 8.0–10.0) or at temperatures ranging from 25 °C to 65 °C. All the assays were performed in triplicate.

Effect of various metal ions (including Ni^{2+}, Mn^{2+}, Mg^{2+}, Fe^{3+}, Ca^{2+}, Zn^{2+}, Al^{3+}, Co^{2+}, Cu^{2+} and Ag^{+}) and EDTA on the activity of Cg26 was determined by addition of each reagent into the reaction mixture at 1.0 mM and incubated at 30 °C for 60 min. The residual activities were measured with 2.0 mM **S25** and 0.5 mM NADPH using the standard protocol. Control experiment was done in the absence of any additives. Effect of different concentrations of Ni^{2+} on the specific activity of purified Cg26 was examined at 0.1, 0.2, 0.5, 1.0, 2.0, and 5.0 mM Ni^{2+} using above described method. All the experiment was conducted in triplicate.

Kinetic constants of the purified Cg26 against **S8**, **S14**, **S15**, **S18**, **S22** and **S25** were determined employing the standard protocol except at various substrate concentrations from 0.1 mM to 10.0 mM. All the assay was performed in triplicate. The apparent K_m, V_{max} and k_{cat} were calculated according to Lineweaver-Burk plot.

2.8. Asymmetric preparation of chiral secondary alcohols using Cg26

Considering the reductases for the preparation of chiral secondary alcohols was NAD(P)$^+$ dependent, glucose dehydrogenase from *Bacillus megaterium* was introduced to regenerate the NAD(P)H and save the cost (Cheng et al., 2016). The co-expressed cells were directly obtained by transferred the plasmids pET28-*Cg26* and pACYCDuet-*gdh* into *E. coli* BL21(DE3). This co-expressed strain was cultivated in LB medium supplemented with kanamycin and chloramphenicol at 50 μg·mL^{-1}, and induced with 0.5 mM IPTG at 25 °C for 6 h. The co-expressed cells were harvested by centrifugation at 8000 × *g* and 4 °C for 10 min, washed with physiological saline, and lyophilized under vacuum using freeze drier (SCIENTZ-10N, Ningbo Scientz Biotechnology Co. Ltd., Ningbo). The powder of co-expressed cells was stored at 4 °C for the asymmetric reduction reaction.

Application potential of Cg26 was evaluated toward two substrates

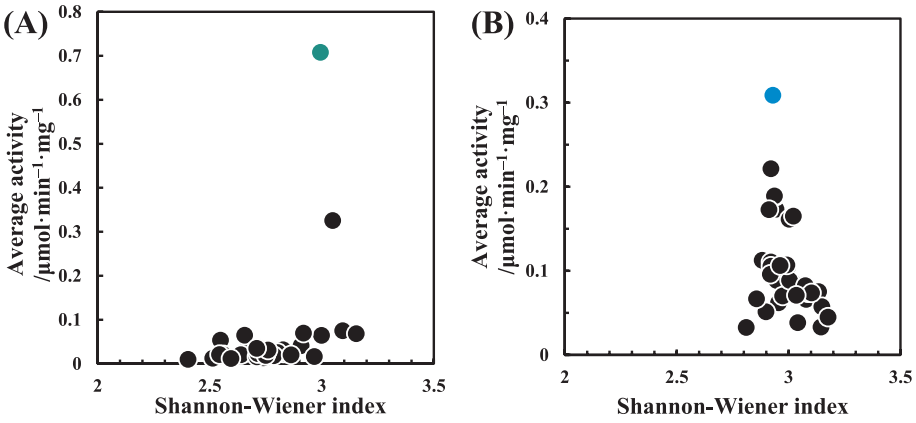

Fig. 2. High throughput screening of *Candida glabrata* hunting library for reductases with high activity and wide substrate spectrum. (A) Using NADPH as cofactor, green dot (●): Cg26. (B) Using NADH as cofactor, blue dot (●): Cg8. Shannon-Wiener index was calculated according to Eq. (2). The specific activities of oxidoreductases toward all the tested substrates were available in the E-supplement. (For interpretation of the references to colour in this figure legend, the reader is referred to the web version of this article.)

(**S8** and **S25**) with the highest specific activities. The 10 mL reaction mixture consisted of co-expressed cells powder (10 g·L^{-1}), different concentrations of **S8** and **S25** from 50 to 200 g·L^{-1}, 1.0 mM Ni^{2+}, and 1.5 equiv. glucose in 10 mL PBS buffer (pH 6.0, 100 mM). The reaction was performed at 30 °C and magnetically stirred at 120 rpm. The pH of the reaction was kept at pH 6.0 by titration with 2.0 M NaOH. At different timer intervals, samples (20 μL) was withdrawn from the reaction mixture and diluted with 480 μL PBS buffer (pH 6.0, 100 mM). Equal volume of ethyl acetate was added, thoroughly mixed and the organic phase was isolated by centrifugation at 12,000*g* for 5 min. The organic phase was dried over anhydrous Na_2SO_4 and analyzed by GC equipped with CP-Chirasil-Dex CB GC Column (25 m × 0.25 mm × 0.25 μm, Agilent) to determine the conversion and enantioselectivity employing previously reported methods (Shen et al., 2012; Xu et al., 2015).

3. Results and discussion

3.1. Development of the genome hunting library of C. glabrata for reductases

Genome hunting and data mining, namely genome mining, are effective and promising strategies for rapid discovery of robust biocatalysts in the post-genomic era (Ni and Xu, 2012). Genome data mining was performed with the sequence of a known biocatalyst as target and by BLAST searching in the whole public database to identify similar proteins with improved properties. Genome hunting was conducted by consensus analysis of the whole genome of a certain microorganism with desired properties. The putative biocatalysts were heterogeneously over-expressed and screened for the desired activity. Genome hunting is more effective compared with traditional purification and shotgun methods, and has been successfully applied in searching for efficient reductases from *S. saccharomyces*, *C. parapsilosis*, *B. subtilis* and cyanobacteria.

Strains of candida genus are important in producing industrial enzymes (Chadha et al., 2016). *Candida glabrata*, belonging to candida genus, has been reported with potentials in synthesis of acetoin, pyruvate, malate and fumarate, and in producing reductases with reducing activity toward ethyl 2-oxo-4-phenylbyrate. Construction and screening the reductases library of *C. glabrata* is supposed to be the most direct and comprehensive approach to study the potential of all putative reductases of *C. glabrata*. Genome of *C. glabrata* had been released under accession no. PRJNA13831 in 2004 with 12.34 Mbp in size and 38.62% GC, 5499 genes and 5213 proteins (Koszul et al., 2003). All the proteins coding genes were analyzed in search for genes with 600–1500 bp in length and NAD(P)H binding motif. Fifty-five putative NAD(P)H-dependent reductases were selected to form the genome hunting library of *C. glabrata*, except for the three reported reductases *Cg*KR1, *Cg*KR2 and *Cg*CR. The information of all the putative reductases coding genes could be found in E-supplement. Phylogenetic analysis revealed that the distinct difference of all the putative reductases.

In order to fully understand the catalytic properties of all the putative reductases, a substrate library was established, whereas in traditional screening only one substrate was tested. A substrate library consists of aliphatic ketone, aliphatic diketone, ketoacid, aromatic ketone, heterocyclic ketone, cyclic ketone, keto ester, aldehyde, nitrile, imine and alkene. As illustrate in Fig. 1, all the substrate could be divided into four subgroups based on the substituents and reducing group, including Group I (**S1–S14**), Group II (**S15–S20**), Group III (**S21–S25**) and Group IV (**S26–S32**). A systematic substrate library could comprehensively reflect the fingerprinting and application potential of tested reductases (Goddard and Reymond, 2004).

3.2. Screening of genome hunting library of C. glabrata for reductases

All 55 putative reductases coding genes were cloned from genomic DNA of *C. glabrata*, ligated into pET28a and transferred into *E. coli* BL21(DE3). After induction with IPTG, the genome hunting library of *C. glabrata* for reductases was established. As analyzed by SDS-PAGE, 37 putative reductases were successfully expressed and migrated at the right position. All of them were mostly or partially expressed in soluble form. Then, the substrate spectrum of above 37 putative reductases were determined toward the substrate library using NADH and NADPH. Average specific activity was adopted to denote the height of the reductases, while Shannon-Wiener index was introduced to reflect the breadth of the reductases. Shannon-Wiener index was a statistic parameter and could be used to display the diversity of the sample. Higher Shannon-Wiener index indicates higher diversity. However, Shannon-Wiener index could be influenced by the number of sample (Liu et al., 2013). As a result, a substrate library containing 32 substrates was developed to evaluate the Shannon-Wiener index of reductases. Based on these, reductases with wide substrate spectrum and high efficiency could be obtained.

Screening result could be seen in Fig. 2. With NADPH as cofactor, most of the reductases displayed average activity lower than 0.1 U·mg^{-1}, and the Shannon-Wiener index was 2.4–3.2. Lower average specific activity might ascribed to the preference to NADH or undesirable activity toward tested substrates, since no background reaction was found with NADPH as cofactor. The reductase Cg26 displayed the highest average specific activity of 0.71 U·mg^{-1} crude enzyme and Shannon-Wiener index of 2.99. With regard to the results with NADH as cofactor, more reductases displayed average specific activity of more than 0.1 U·mg^{-1}, and the Shannon-Wiener index was 2.8–3.3. Activities of most reductases toward tested substrates were low and at similar level using NADH as cofactor. As a result, the Shannon-Wiener index was higher than that using NADPH as cofactor. The average specific activity of reductase Cg8 was 0.31 U·mg^{-1}, ranking the highest. The Shannon-Wiener index of reductase Cg8 was 2.93. Considering their higher average activity and Shannon-Wiener index,

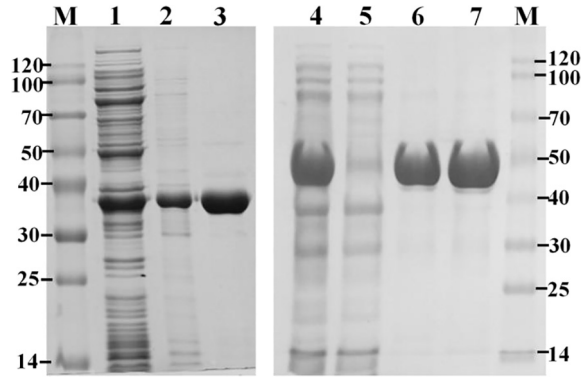

Fig. 3. SDS-PAGE analysis of purified Cg8 and Cg26. Lanes 1 & 2: supernatant and precipitant parts of Cg8, Lane 3: purified Cg8, Lanes 4 & 5: supernatant and precipitant parts of Cg26, Lane 6 & 7: purified Cg26, Lane M: protein molecular marker.

reductases Cg8 and Cg26 were chosen for further study.

3.3. Characterization of Cg8 and Cg26

Recombinant Cg8 and Cg26 were purified to homogeneity by nickel affinity chromatography to investigate the enzymatic properties. As shown in Fig. 3, reductase Cg8 was partially soluble expressed, while reductase Cg26 was mostly soluble expressed. Purified reductases Cg8 and Cg26 were migrated as a single band at about 36 and 46 kDa respectively. Sequence alignment and classification of Cg8 and Cg26 were also carried out. Reductases Cg8 and Cg26 are comprised of 294 and 348 residues respectively. Cg8 belongs to short chain dehydrogenase/reductase (SDR) superfamily according to the SDR HMM library (Persson et al., 2009), and possessed the catalytic triad of Ser142-Tyr155-Lys159. BLASTp search in the NCBI database revealed that Cg8 has the highest identity of 35% with dehydrogenase from fungal *Rhizobium etli* (PDB no. 4FGS). Cg26 is also classified into SDR superfamily. The catalytic triad of Cg26 was Ser181-Tyr203-Lys207. Cg26 displays low sequence identify (< 20%) to other reported carbonyl reductases.

Although both Cg8 and Cg26 belong to SDR superfamily, low sequence identity of 15.3% was observed between them according to the multiple sequence alignment. SDR superfamily is a very large class of enzymes and could be divided into five families based on the sequence length and conserved residues, including 'divergent', 'classical', 'intermediate', 'extended' and 'complex'. Classical SDRs are typically about 250 residues long, while extended SDRs are approximately 350 residues (Kallberg et al., 2002). As shown in Table 1, Cg8 and Cg26 belonged to 'classical' and 'extended' families respectively, since they possessed all the conserved elements, including coenzyme binding motif, motif for stabilizing central *β*-sheet and active sites.

Substrate fingerprinting of purified Cg8 and Cg26 was also determined as illustrated in Fig. 4 and Table 2. Cg8 displayed the highest specific activity toward 3-quinuclidone (**S19**, 23.7 U·mg^{-1}), while Cg26 preferred 2,4′-„dichloroacetophenone (**S8**, 49.0 U·mg^{-1}). The average activity and Shannon-Wiener index of Cg8 and Cg26 were 4.04 U·mg^{-1} and 2.78, 8.95 U·mg^{-1} and 2.82. Cg26 had higher activity and wider substrate spectrum than Cg8. It can also be found that they exhibited different substrate preference. Average activity and Shannon-Wiener index against four groups of substrates were also calculated. Cg26 displayed higher activity (16.5 U·mg^{-1}) toward Group III (keto esters), while Cg8 displayed higher average activity (8.50 U·mg^{-1}) toward Group II (cyclic ketones). Both Cg8 and Cg26 showed the highest Shannon-Wiener index toward Group I (aliphatic and aromatic ketones), which indicate that the difference in activity toward Group I substrates is not distinct. Besides Group I, Cg26 exhibited higher Shannon-Wiener index (0.70) toward Group III, while Cg8 exhibited higher Shannon-Wiener index (0.90) toward Group II. Both of them displayed the lowest activity toward Group IV substrates. Consequently, Cg26 is more efficient than Cg8 in the reduction of all the tested substrates. Furthermore, enzymatic properties and application of Cg26 in the potential synthesis of chiral alcohols were evaluated.

3.4. Enzymatic properties of purified Cg26

In order to apply this newly identified Cg26 in the preparation of chiral secondary alcohols, enzymatic properties was examined with ethyl 2-oxo-4-phenylbutyrate (**S25**) as substrate. The optimum pH and temperature were determined to be pH 5.0 and 50 °C as shown in E-supplement. Metal ions dependence revealed that addition of EDTA could severely reduce the activity of Cg26, and only 19.4% activity was reserved, indicating the activity of Cg26 might be dependent on metal ions. Divalent cations Ni^{2+}, Mn^{2+}, Mg^{2+}, Fe^{2+} and Ca^{2+} could improve the activity of Cg26 to 148%, 141%, 141%, 120%, and 109% respectively, while Cu^{2+} and Ag^{+} could deactivate Cg26 with residual activity of 4.09% and 0.72. The relative activity of Cg26 at 0.1, 0.2, 0.5, 1.0, 2.0, and 5.0 mM Ni^{2+} was 118%, 129%, 147%, 148%, 148%, and 134% respectively. Cg26 displayed the highest activity at Ni^{2+} concentrations ranging from 0.5 to 2.0 mM. As a result, Cg26 is metal ions dependent and 1.0 mM Ni^{2+} was supplemented in the further experiment.

Kinetic parameters of purified Cg26 toward six preferred substrates, including 2,4′-„dichlroracetophenone (**S8**), 2-(4′-„chlorobenzoyl)-pyridine (**S14**), 4-ethylcyclohexanone (**S15**), dihydro-3-thiophenone (**S18**), ethyl 4-chloroacetoacetate (**S22**) and ethyl 2-oxo-4-phenylbutyrate (**S25**) were determined (Table 3). The K_m and k_{cat} of Cg26 toward them were 0.75 mM and 36.7 s^{-1}, 5.63 mM and 5.11 s^{-1}, 1.42 mM and 9.05 s^{-1}, 7.39 mM and 12.1 s^{-1}, 2.24 mM and 5.53 s^{-1}, and 0.50 mM and 29.7 s^{-1} respectively. Cg26 exhibited the highest k_{cat}/K_m of 59.4 s^{-1}·mM^{-1} toward **S25**, whose product could be used as vital building blocks of angiotensin-converting enzyme (ACE) inhibitors, such as benazepril and ramipril etc, for treatment of hypertension and congestive heart failure. The K_m of Cg26 was at moderate level (Ni et al., 2013) among various OPBE reductase which is over a range from 0.1 mM to 20.1 mM. In comparison with *Cg*KR2, Cg26 displayed higher specific activity and k_{cat} toward **S25**, which were 10.6 U·mg^{-1} and 11.0 s^{-1} (Shen et al., 2012).

3.5. Asymmetric preparation of secondary alcohols using recombinant Cg26

Since reductases are dependent on NAD(P)H, cofactor regeneration

Table 1
Secondary structure element motifs of 'classical' and 'extended' SDR in Cg8 and Cg26.

Secondary structure element	Classical	Cg8	Extended	Cg26	Function
β1 + α1	TGxxxGhG	TGASSGIG	TGxx[GS]phG	TGANSNLG	Coenzyme binding region
β3 + α3	Dhx[cp]	DISE	DhxD	DFD	Adenine ring binding of coenzyme
β4	hDhhhNNAG	LDILYNNAG	[DE]xxxxhhhxAA	ESINYFFVNAA	Structural role in stabilizing central β-sheet
β5	GxhhxxhSh	GTVIFTGSI	hhhxSSxxh	VVWISSIMA	Part of active site
α5	Yx[AS][ST]K	YAATK	Yxx[AS]K	YEGSK	Part of active site

Note: 'c' denotes a charged residue, 'h' denotes a hydrophobic residue, 'p' denotes a polar residue and 'x' denotes any residue or gap. Conserved amino acids are underlined. Alternative amino acids at a motif position are given within brackets.

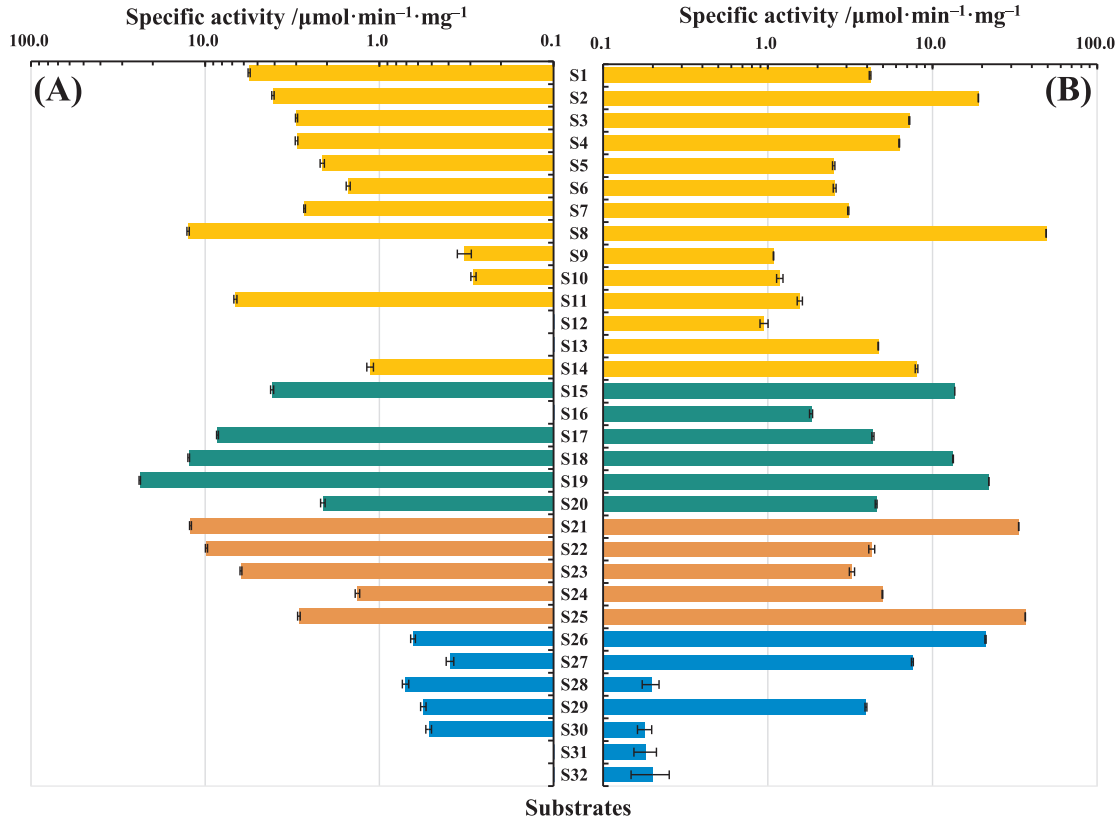

Fig. 4. Substrate fingerprints of purified Cg8 and Cg26 toward diverse substrates. (A): Cg8, (B): Cg26. (): Group I substrates, (); Group II substrates; (): Group III substrates, (): Group IV substrates.

Table 2
Comparison of substrate fingerprint characterization parameters of Cg8 and Cg26.

Entry		Cg8	Cg26
Best substrate		**S19**	**S8**
Highest activity /μmol·min^{-1}·mg^{-1}		23.7 ± 0.22	49.0 ± 0.07
Average activity /μmol·min^{-1}·mg^{-1}		4.04	8.95
Shannon-Wiener index		2.78	2.82
Group I	Average activity /μmol·min^{-1}·mg^{-1}	3.07	7.94
	Shannon-Wiener index	2.12	1.91
Group II	Average activity /μmol·min^{-1}·mg^{-1}	8.50	9.93
	Shannon-Wiener index	1.14	1.20
Group III	Average activity /μmol·min^{-1}·mg^{-1}	6.50	16.5
	Shannon-Wiener index	1.39	1.18
Group IV	Average activity /μmol·min^{-1}·mg^{-1}	0.41	4.74
	Shannon-Wiener index	1.63	1.00

Table 3
Kinetic parameters of purified Cg26 toward prochiral ketones.

Entry	Substrate	K_m [mM]	k_{cat} [s^{-1}]	k_{cat}/K_m [s^{-1}·mM^{-1}]
1	2,4′-Dichloroacetophenone, **S8**	0.75 ± 0.05	36.7 ± 0.8	48.9
2	2-(4′-Chlorobenzoyl)-pyridine, **S14**	5.63 ± 0.15	5.11 ± 0.13	0.91
3	4-Ethylcylohexanone, **S15**	1.42 ± 0.08	9.05 ± 0.21	6.37
4	Dihydro-3-thiophenone, **S18**	7.39 ± 0.13	12.1 ± 0.2	1.64
5	Ethyl 4-chloroacetoacetate, **S22**	2.24 ± 0.08	5.53 ± 0.19	2.47
6	Ethyl 2-oxo-4-phenylbutyrate, **S25**	0.50 ± 0.06	29.7 ± 0.8	59.4

was introduced to reduce the cost of NAD(P)$^+$. In our previous work, glucose dehydrogenase (GDH) from *Bacillus subtilis* was identified and inserted into pACYCDuet (Cheng et al., 2016). Co-expression of Cg26 and GDH was constructed by simultaneous transferring pET28-*cg26* and pACYCDuet-*gdh* into *E. coli* BL21(DE3). The potential of Cg26 in the preparation of chiral secondary alcohols was investigated by employing this co-expression strain. Although the highest activity of purified Cg26 was detected at pH 5.0, the buffer employed in the asymmetric reaction was PBS (pH 6.0, 100 mM), in the view of balancing the activity of Cg26 and GDH since the activity of GDH was low and the cofactor was not stable at pH 5.0. Considering its highest k_{cat}/K_m value toward **S8** and **S25**, asymmetric reduction of these two substrates was evaluated at 50, 100, 150 and 200 g·L^{-1} substrate loadings and 10 g·L^{-1} co-expressed cells.

As shown in Fig. 5A, 50 g·L^{-1} **S8** could be completely reduced into (*R*)-(2,4′)-dichloroacetophenol with 99.9% *e.e.* at 8 h, and 100 g·L^{-1} **S8** could be fully reduced at 12 h with 98.7% *e.e.*. The enantioselectivity was slightly reduced along with the increase loading of **S8**, suggesting the toxicity of **S8** might affect the activity and enantioselectivity of reductases (Xie et al., 2010). Further increase the concentration to 150 g·L^{-1}, conversion of **S8** could reach 99.1% at 24 h, however the *e.e.* was further decreased to 97.4%. As a result, the reduction of **S8** at 200 g·L^{-1} was not tested. The substrate to biocatalyst was *c.a.* 15 at 150 g·L^{-1} **S8**.

Asymmetric reduction of **S25** was also investigated at various substrate loadings (Fig. 5B). At first, 50 g·L^{-1} **S25** could be quickly reduced into ethyl (*R*)-2-hydroxy-4-phenylbutyrate ((*R*)-HPBE) in 2 h with 99.5% conversion and > 99.9% *e.e.*. The highest k_{cat}/K_m value of Cg26 toward **S25** might account for its excellent performance. Further increasing **S25** loading to 100 and 150 g·L^{-1}, high reaction rate was maintained, and the substrate could be depleted within 8 h and 12 h respectively. Most importantly, the enantioselectivity was not influenced at increased substrate loadings. However, when further increased

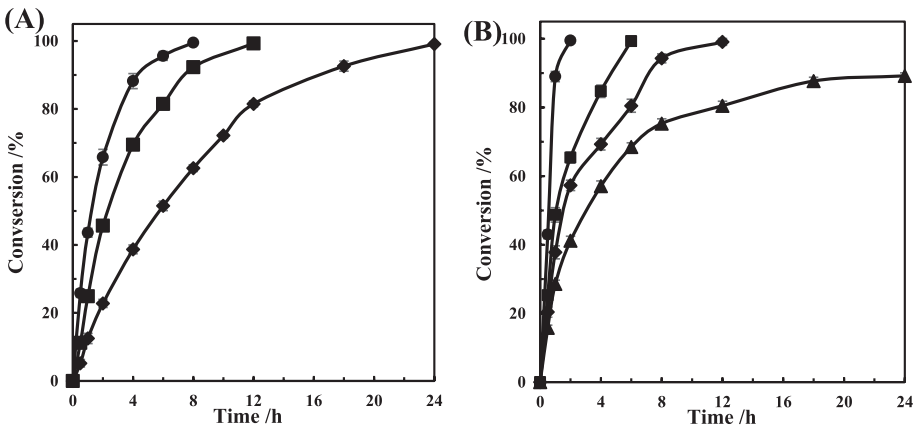

Fig. 5. Asymmetric reduction of **S8** and **S25** using recombinant Cg26. (A): **S8**, (B): **S25**. (●): 50 g·L^{-1}, (■): 100 g·L^{-1}, (♦): 150 g·L^{-1}, (▲): 200 g·L^{-1}.

to 200 g·L^{-1}, only 89.2% of **S25** was converted into product with > 99.9% *e.e.*. Catalyzed by 10 g·L^{-1} of Cg26, as much as 150 g·L^{-1} **S25** could be fully reduced into (*R*)-HPBE with substrate to biocatalyst ratio of 15, space-time yield of *c.a.* 300 g·L^{-1}·d^{-1}, and > 99.9% *e.e.*. Corresponding alcohol product of **S25** was isolated and verified to be (*R*)-HPBE by NMR. ^{1}H NMR ($CDCl_3$, 400 MHz): δ 1.29 (3H, t, OCH_2CH_3), δ 1.90–1.99 (1H, m, $ArCH_2CHH$), δ 2.07–2.16 (1H, m, $ArCH_2CHH$), δ 2.73–2.79 (2H, m, $ArCH_2$), δ 3.14 (1H, s, OH), δ 4.16–4.22 (3H, m, OCH_2CH_3, CHOH), δ 7.16–7.29 (5H, m, Ar-H). ^{13}C NMR ($CDCl_3$, 100 MHz): δ14.11, 30.96, 35.90, 61.64, 69.63, 125.94, 128.37, 141.13, 175.14.

In the batch reaction without substrate feeding for the preparation of (*R*)-HPBE, the highest substrate to biocatalyst ratio was 4.12, obtained by CgKR2 at 206 g·L^{-1} **S25**, 20 g·L^{-1} biocatalyst loading and 0.05 mM NADPH (Shen et al., 2012). This Cg26 displayed the highest substrate to biocatalyst ratio in the asymmetric reduction of **S25** than previously reported processes. Further optimization of the biocatalytic reaction (such as substrate feeding, etc) might further improve the performance of Cg26 in the preparation of chiral secondary alcohols (Ni et al., 2013). Besides that, various chiral secondary alcohols would be synthesized employing specific reductases of *C. glabrata* according to the result of substrate fingerprints analysis.

4. Conclusions

In this study, genome hunting library of *Candida glabrata* was developed to search for reductases with promising potentials in preparation of chiral secondary alcohols. The height and breadth of each reductases in activity were calculated by average specific activity and Shannon-Wiener index. Cg26 were identified with average activity of 8.95 U·mg^{-1} and Shannon-Wiener index of 2.82. Ethyl 2-oxo-4-phenylbutyrate loading of 150 g·L^{-1} could be completely converted into ethyl (*R*)-2-hydroxy-4-phenylbutyrate at expense of 10 g·L^{-1} Cg26. This study provides evidence for screening and application of reductases from *C. glabrata* in the preparation of chiral secondary alcohols.

Acknowledgement

We are grateful to the National Natural Science Foundation of China (21506073, 21776112), the Natural Science Foundation of Jiangsu Province (BK20150003, BK20171135), Six talent peaks project of Jiangsu Province (2015-SWYY-008), the Program of Introducing Talents of Discipline to Universities (111-2-06), and a project funded by the Priority Academic Program Development of Jiangsu Higher Education Institutions for the financial support of this research.

Appendix A. Supplementary data

Supplementary data associated with this article can be found, in the online version, at http://dx.doi.org/10.1016/j.biortech.2017.09.111.

References

Bornscheuer, U.T., Huisman, G.W., Kazlauskas, R.J., Lutz, S., Moore, J.C., Robins, K., 2012. Engineering the third wave of biocatalysis. Nature 485, 185–194.
Chadha, A., Venkataraman, S., Preetha, R., Padhi, S.K., 2016. *Candida parapsilosis*: a versatile biocatalyst for organic oxidation-reduction reactions. Bioorg. Chem. 68, 187–213.
Chen, X.L., Wu, J., Song, W., Zhang, L.M., Wang, H.J., Liu, L.M., 2015. Fumaric acid production by *Torulopsis glabrata*: engineering the urea cycle and the purine nucleotide cycle. Biotechnol. Bioeng. 112, 156–167.
Chen, X.L., Xu, G.Q., Xu, N., Zou, W., Zhu, P., Liu, L.M., Chen, J., 2013. Metabolic engineering of *Torulopsis glabrata* for malate production. Metab. Eng. 19, 10–16.
Cheng, J., Xu, G.C., Han, R.Z., Dong, J.J., Ni, Y., 2016. Efficient access to L-phenylglycine using a newly identified amino acid dehydrogenase from Bacillus clausii. RSC Adv. 6, 80557–80563.
Fu, Y.L., Castiglione, K., Weuster-Botz, D., 2013. Comparative characterization of novel ene-reductases from cyanobacteria. Biotechnol. Bioeng. 110, 1293–1301.
Goddard, J.P., Reymond, J.L., 2004. Enzyme activity fingerprinting with substrate cocktails. J. Am. Chem. Soc. 126, 11116–11117.
Goldberg, K., Schroer, K., Lütz, S., Liese, A., 2007. Biocatalytic ketone reduction-a powerful tool for the production of chiral alcohols-part I: processes with isolated enzymes. Appl. Microbiol. Biotechnol. 6, 237–248.
Huisman, G.W., Liang, J., Krebber, A., 2010. Practical chiral alcohol manufacture using ketoreductases. Curr. Opin. Chem. Biol. 14, 122–129.
Itoh, N., 2014. Use of the anti-prelog stereospecific alcohol dehydrogenase from leifsonia and pseudomonas for producing chiral alcohols. Appl. Microbiol. Biotechnol. 98, 3889–3904.
Kallberg, Y., Oppermann, U., Jörnvall, H., Persson, B., 2002. Short-chain dehydrogenases/reductases (SDRs) – coenzyme-based functional assignments in completed genomes. Eur. J. Biochem. 269, 4409–4417.
Kaluzna, I.A., Matsuda, T., Sewell, A.K., Stewart, J.D., 2004. Systematic investigation of *Saccharomyces cerevisiae* enzymes catalyzing carbonyl reductions. J. Am. Chem. Soc. 12827–12832.
Koszul, R., Malpertuy, A., Frangeul, L., Bouchier, C., Wincker, P., Thierry, A., Duthoy, S., Ferris, S., Hennequin, C., Dujon, B., 2003. The complete mitochondrial genome sequence of the pathogenic yeast *Candida* (Torulopsis) glabrata. FEBS Lett. 534, 39–48.
Kroutil, W., Mang, H., Edegger, K., Faber, K., 2004. Recent advances in the biocatalytic reduction of ketones and oxidation of *sec*-alcohols. Curr. Opin. Chem. Biol. 8, 120–125.
Li, S.B., Liu, L.M., Chen, J., 2015. Compartmentalizing metabolic pathway in *Candida glabrata* for acetoin production. Metab. Eng. 28, 1–7.
Li, Y., Chen, J., Lun, S.Y., 2001. Biotechnological production of pyruvic acid. Appl. Microbiol. Biotechnol. 57, 451–459.
Liu, J.Y., Zheng, G.W., Li, C.X., Yu, H.L., Pan, J., Xu, J.H., 2013. Multi-substrate fingerprinting of esterolytic enzymes with a group of acetylated alcohols and statistic analysis of substrate spectrum. J. Mol. Catal. B: Enzym. 89, 41–47.
Ma, H.M., Yang, L.L., Ni, Y., Zhang, J., Li, C.X., Zheng, G.W., Yang, H.Y., Xu, J.H., 2012. Stereospecific reduction of methyl o-chlorobenzoylformate at 300 g·L^{-1} without additional cofactor using a carbonyl reductase mined from *Candida glabrata*. Adv. Synth. Catal. 354, 1765–1772.
Matsuda, T., Yamanaka, R., Nakamura, K., 2009. Recent progress in biocatalysis for asymmetric oxidation and reduction. Tetrahedron: Asymmetry 20, 513–557.
Ni, Y., Li, C.X., Ma, H.M., Zhang, J., Xu, J.H., 2011. Biocatalytic properties of a recombinant aldo-keto reductase with broad substrate spectrum and excellent stereoselectivity. Appl. Microbiol. Biotechnol. 89, 1111–1118.
Ni, Y., Su, Y.N., Li, H.D., Zhou, J.Y., Sun, Z.H., 2013. Scalable biocatalytic synthesis of optically pure ethyl (*R*)-2-hydroxy-4-phenylbutyrate using a recombinant *E. coli* with high catalyst yield. J. Biotechnol. 168, 493–498.
Ni, Y., Xu, J.H., 2012. Biocatalytic ketone reduction: a green and efficient access to enantiopure alcohols. Biotechnol. Adv. 30, 1279–1288.
Nie, Y., Xiao, R., Xu, Y., Montelione, G.T., 2011. Novel anti-Prelog stereospecific carbonyl

reductases from *Candida parapsilosis* for asymmetric reduction of prochiral ketones. Org. Biomol. Chem. 9, 4070–4078.
Otto, C., Yovkova, V., Barth, G., 2011. Overproduction and secretion of alpha-ketoglutaric acid by microorganisms. Appl. Microbiol. Biotechnol. 92, 689–695.
Persson, B., Kallberg, Y., Bray, J.E., Bruford, E., Dellaporta, S.L., Favia, A.D., Duarte, R.G., Jörnvall, H., Kavanagh, K.L., Kedishvili, N., Kisiela, M., Maser, E., Mindnich, R., Orchard, S., Penning, T.M., Thornton, J.M., Adamski, J., Oppermann, U., 2009. The SDR (short-chain dehydrogenase/reductase and related enzymes) nomenclature initiative. Chem. Biol. Interact. 178, 94–98.
Shen, N.D., Ni, Y., Ma, H.M., Wang, L.J., Li, C.X., Zheng, G.W., Zhang, J., Xu, J.H., 2012. Efficient synthesis of a chiral precursor for angiotensin-converting enzyme (ACE) inhibitors in high space-time yield by a new reductase without external cofactors. Org. Lett. 14, 1982–1985.
Xie, Y., Xu, J.H., Xu, Y., 2010. Isolation of a *Bacillus* strain producing ketone reductase with high substrate tolerance. Bioresour. Technol. 101, 1054–1059.
Xu, G.C., Yu, H.L., Shang, Y.P., Xu, J.H., 2015. Enantioselective bioreductive preparation of chiral halohydrins employing two newly identified stereocomplementary reductases. RSC Adv. 5, 22703–22711.
Zhang, W., Ni, Y., Sun, Z.H., Zheng, P., Lin, W.Q., Zhu, P., Ju, N.F., 2009. Biocatalytic synthesis of ethyl (*R*)-2-hydroxy-4-phenylbutyrate with *Candida krusei* SW2026: a practical process for high enantiopurity and product titer. Process Biochem. 44, 1270–1275.
Zheng, G.W., Xu, J.H., 2011. New opportunities for biocatalysis: driving the synthesis of chiral chemicals. Curr. Opin. Biotechnol. 22, 784–792.
Zheng, Y.G., Yin, H.H., Yu, D.F., Chen, X., Tang, X.L., Zhang, X.J., Xue, Y.P., Wang, Y.J., Liu, Z.Q., 2017. Recent advances in biotechnological applications of alcohol dehydrogenases. Appl. Microbiol. Biotechnol. 101, 987–1001.